Journal of Quantitative Spectroscopy & Radiative Transfer 253 (2020) 107105

Contents lists available at ScienceDirect

Journal of Quantitative Spectroscopy & Radiative Transfer

journal homepage: www.elsevier.com/locate/jqsrt

# The far-infrared spectrum of $^{18}O$ enriched water vapour (40–700 $cm^{-1}$)

S.N. Mikhailenko[a], S. Béguier[b], T.A. Odintsova[c], M.Yu. Tretyakov[c], O. Pirali[d,e], A. Campargue[b,*]

[a] V.E. Zuev Institute of Atmospheric Optics, SB, Russian Academy of Science, 1, Academician Zuev square, 634055 Tomsk, Russia
[b] Univ. Grenoble Alpes, CNRS, LIPhy, 38000 Grenoble, France
[c] Institute of Applied Physics, Russian Academy of Sciences, Nizhniy Novgorod, Russia
[d] SOLEIL Synchrotron, L'Orme des Merisiers, Saint-Aubin 91192, Gif-Sur-Yvette, France
[e] Université Paris-Saclay, CNRS, Institut des Sciences Moléculaires d'Orsay, 91405 Orsay, France

ARTICLE INFO

*Article history:*
Received 29 April 2020
Revised 19 May 2020
Accepted 19 May 2020
Available online 13 June 2020

*Keywords:*
Water vapour
Far-infrared
Rotational spectrum
Water isotope

ABSTRACT

The rotational spectrum of water vapour highly enriched in $^{18}O$ has been studied by high resolution (≈ 0.001 $cm^{-1}$) Fourier transform spectroscopy at the AILES beam line of the SOLEIL synchrotron. The room temperature absorption spectrum has been recorded between 40 and 700 $cm^{-1}$. The $^{18}O$ enrichment of the sample was about 97% while the gas pressure and the absorption pathlength were set to 0.97 mbar and 151.75 m, respectively. The spectrum contains more than 4800 rotational transitions from seven water isotopologues ($H_2{}^{18}O$, $H_2{}^{16}O$, $H_2{}^{17}O$, $HD^{18}O$, $HD^{16}O$, $HD^{17}O$, $D_2{}^{18}O$). The assignments were performed using known experimental energy levels as well as calculated line lists based on the results of Schwenke and Partridge. The amount and accuracy of the reported line positions represent an important extension compared to previous works. Overall, lines of about 2570 transitions are observed for the first time and 35, 41, 50, and 16 new energy levels are determined for $H_2{}^{18}O$, $H_2{}^{17}O$, $HD^{18}O$, and $HD^{17}O$, respectively. The set of derived energy levels shows a number of important differences from those recommended by an IUPAC-task group. Compared to the HITRAN2016 database, numerous deviations of line positions (up to 0.15 $cm^{-1}$) are found for the $H_2{}^{17}O$, $H_2{}^{18}O$, $HD^{17}O$, and $HD^{18}O$ species. Incomplete and wrong HITRAN's assignments of more than 90 transitions for $H_2{}^{18}O$, $H_2{}^{17}O$ and $HD^{18}O$ are identified. Overall, the measured line positions will allow to significantly refine and complete the sets of empirical energy levels of $H_2{}^{18}O$, $H_2{}^{17}O$, $HD^{18}O$ and $HD^{17}O$ in the ground vibrational state.

© 2020 Elsevier Ltd. All rights reserved.

## 1. Introduction

Water vapour plays a crucial role in the Earth's radiation budget determining our climate [1]. For instance, the water distribution over the globe is permanently monitored by satellite based remote sensing instruments [2]. In this context, a very accurate knowledge of water vapour absorption is required for a wide variety of applications in geoscience [3]. This applies to the main isotopologue, $H_2{}^{16}O$, but also to the less abundant $H_2{}^{18}O$, $H_2{}^{17}O$ and $HD^{18}O$ species (Note that only $CO_2$ is more abundant than $H_2{}^{18}O$ in the Earth atmosphere). Indeed, quantitative information on the natural variation of isotopic abundance ratios, measured by absorption methods, is currently used to trace various chemical and physical atmospheric processes (*e.g.* [4]). Note that a complete and accurate line list of the water monomer, including line profile parameters, is also a prerequisite for a reliable determination of the atmospheric continuum absorption, which is one of the oldest and the long-standing problem in molecular spectroscopy (*e.g.*, review papers [5–7] and references therein).

In the recent decades, new approaches to the calculation of vibration-rotation energy levels have been developed up to the first dissociation limit (*e.g.* [8–11]). In general, theoretical line lists show important advantages in terms of completeness, and quality of line intensity predictions. As concerns line positions, theory does not yet compete with the experimental accuracy achieved using high resolution spectrometers. As a result, recommended line lists for water vapour combine the advantages of experimental and theoretical tools, calculated line positions being adjusted according to experimentally determined energy levels. This method is that adopted for a large fraction of the water line list provided by the HITRAN [12] and GEISA [13] databases.

* Corresponding author.
*E-mail address:* alain.campargue@univ-grenoble-alpes.fr (A. Campargue).

https://doi.org/10.1016/j.jqsrt.2020.107105
0022-4073/© 2020 Elsevier Ltd. All rights reserved.

The present work is devoted to an experimental study of the absorption spectrum of water vapour in the far-IR region, below 700 $cm^{-1}$. It is commonly believed that the rotational transitions involving the lowest vibrational states of light atmospheric molecules are sufficiently well known and characterized. The results reported in this work indicate that a broad-band high resolution and high sensitivity recording of water vapour spectrum in the far-IR range allows for a substantial extension of the previous knowledge in the region. We believe that the main reason of the revealed information shortage in the THz and far-IR spectral ranges (a region that we define as 1–15 THz or 30–500 $cm^{-1}$), is the insufficient performances of laboratory spectrometers. While important technological progresses boosted the performances of spectroscopic instruments in the microwave and IR domains in terms of frequency metrology, accessible bandwidth, and sensitivity, the THz/far-IR lacks spectrometers allowing broadband surveys with MHz-level spectral resolution. In the past decades, due to the atmospheric importance of water vapour, several (and often unique) set-ups were applied to the far-IR spectroscopy of water vapour isotopologues [14–40]. They provided valuable although incomplete set of observations with, in general, limited quality in terms of accuracy and sensitivity. Fourier-Transform instruments, with improved spectral resolution over the years, exploited the relatively weak far-IR continuum from globar and/or mercury lamps to record absorption spectra of water isotopologues [14–17,19,21,33,34,38]. These recordings provided important survey data but with limited frequency and intensity accuracy. In addition to absorption spectroscopy, the frequencies of rotation transitions involving the ground and several excited vibrational states of $H_2O$ could be measured using various emission set-ups associated with FT interferometers [27–31,37,39,40].

In order to improve the frequency accuracy of spectroscopic measurements in the far-IR, several original instruments have been developed in late 90′s. In particular, Evensons' type tunable far-IR spectrometers [41], whose principle is based on the mixing of two frequency stabilized $CO_2$ laser lines separated by few THz, allowed to record absorption spectra with few hundred kHz spectral resolution. Using this instrumental approach, the Toyama University group was able to produce several highly accurate line lists of water and its isotopologues in the 1–5 THz range [18,24,36]. In a similar context, Yu et al. [32] reported a combined analysis of highly accurate absorption spectra recorded with frequency multiplication chains (up to 2.7 THz) together with a broadband far-IR FT emission spectra.

Recently, the advent of few beam lines extracting the far-IR radiation from synchrotron facilities allowed for recording Fourier transform spectra with much higher SNR than with the conventional blackbody sources [23,32,42], despite a spectral resolution inherently limited to about 30 MHz for commercial instruments. The increased sensitivity of these set-ups allowed for the detection of relatively weak signals as shown in our recent measurements of the far-IR water continuum absorption [43,44], or the pure rotation spectrum of $O_2$ [45]. In the present study, we used the experimental set-up developed on the AILES beam line of the synchrotron SOLEIL to extensively improve the far-IR dataset of water isotopic species providing new frequency standards for these important molecules.

The paper is organized as follows. In Section, II we present experimental details including the spectrum acquisition and line list construction. The assignment of observed transitions is presented in Section III. Comparison of our data with previously known information and closing remarks are given in Section IV and V, respectively.

## 2. Experiment

The Fourier-transform absorption spectrum of $^{18}O$ enriched water vapour was recorded in the 40 – 700 $cm^{-1}$ region on the AILES beam line of SOLEIL synchrotron facility. The recordings were performed during a measurement campaign devoted to the study of the far-IR water vapour self-continuum absorption [43]. The continuum measurements were obtained using both water in natural isotopic abundance and with a highly enriched $^{18}O$ sample (the impact of such isotopic substitution upon the water self-continuum might give insights on the physical nature of the water continuum). Note that the continuum retrieval from the measured absorption requires the subtraction of the monomer contribution and thus an accurate and complete line list of water monomer lines in the region.

In the present work, the cell was filled with $^{18}O$ enriched water vapour (97% enrichment from Eurisotop) at a pressure of 0.98 mbar measured by a capacitance gauge (Pfeiffer 10 mbar full range with corresponding accuracy of 0.01 mbar). The resolution (defined as 0.9/MOPD where MOPD = 882 cm is the maximum optical path difference) was set to 0.00102 $cm^{-1}$ in Bruker' definition and no apodization of the interferogram was used (boxcar option of the Bruker software). The spectra were recorded in the 40–700 $cm^{-1}$ spectral range using the SOLEIL synchrotron radiation in standard mode, together with a 4 K cooled Si bolometer detector and a 6 µm mylar-composite beam splitter. The absorption spectra were obtained using a multipass cell in White-type configuration. The total absorption path length was set to 151.75 ± 1.5 m corresponding to 60 passes between mirrors separated by 2.52 m and about 0.5 m of space between the 50 µm thick polypropylene films windows. The spectrum was recorded at room temperature (298.0(3) K), that was monitored by a pair of platinum sensors mounted on the cell external surface. Two hundred spectra corresponding to a recording time of 10 h were co-added. An overview of the transmittance spectrum is displayed on the upper panel of **Fig. 1**, which includes successive zooms. The absorption coefficient was determined as $\alpha_{total} = 1/L \ln(I_0(\nu)/I(\nu))$, where $I(\nu)$ and $I_0(\nu)$ correspond to the spectrum recorded with the cell filled with water vapour and evacuated, respectively.

The absolute frequency calibration was performed by frequency matching of 380 measured line centers of intermediate intensities with accurate $H_2{}^{16}O$ line positions from Refs. [17–19,23,24,26,32]. As a result of the calibration procedure, the statistical uncertainty of the line centers is estimated to vary from $3 \times 10^{-5}$ to $1 \times 10^{-4}$ $cm^{-1}$ over the 50–700 $cm^{-1}$ range of the recordings. Note that, at the recording pressure of 0.98 mbar, the amplitude of the water line pressure shifts may reach 0.1 $cm^{-1}$/atm for the lowest $J = 0$ and 1 transitions. For these lines we recommend increasing the evaluated uncertainty up to $2 \times 10^{-4}$ $cm^{-1}$ until accurate data on line shift coefficients become available. For larger $J$ values, the shift magnitude decreases and thus a total uncertainty of $1 \times 10^{-4}$ $cm^{-1}$ is believed to be a conservative estimate.

The line parameters retrieval was performed using a home-made multiline fitting program in LabVIEW and C++. In our pressure conditions, the pressure broadening (about $4 \times 10^{-4}$ $cm^{-1}$ HWHM at 1 mbar [12]), the Doppler broadening (on the order of $1.5 \times 10^{-4}$ $cm^{-1}$ near 100 $cm^{-1}$) and the apparatus function (about $3.5 \times 10^{-4}$ $cm^{-1}$ HWHM) contribute significantly to the line profile. The present study being mainly focused on line positions, the FTS transmittance spectrum was fitted assuming the standard Voigt line profile as line shape. As starting point of the fit, an empirical line list including line profile parameters was prepared mainly on the basis of the HITRAN database [12], intensity values being scaled according to estimated values of the isotopic abun-

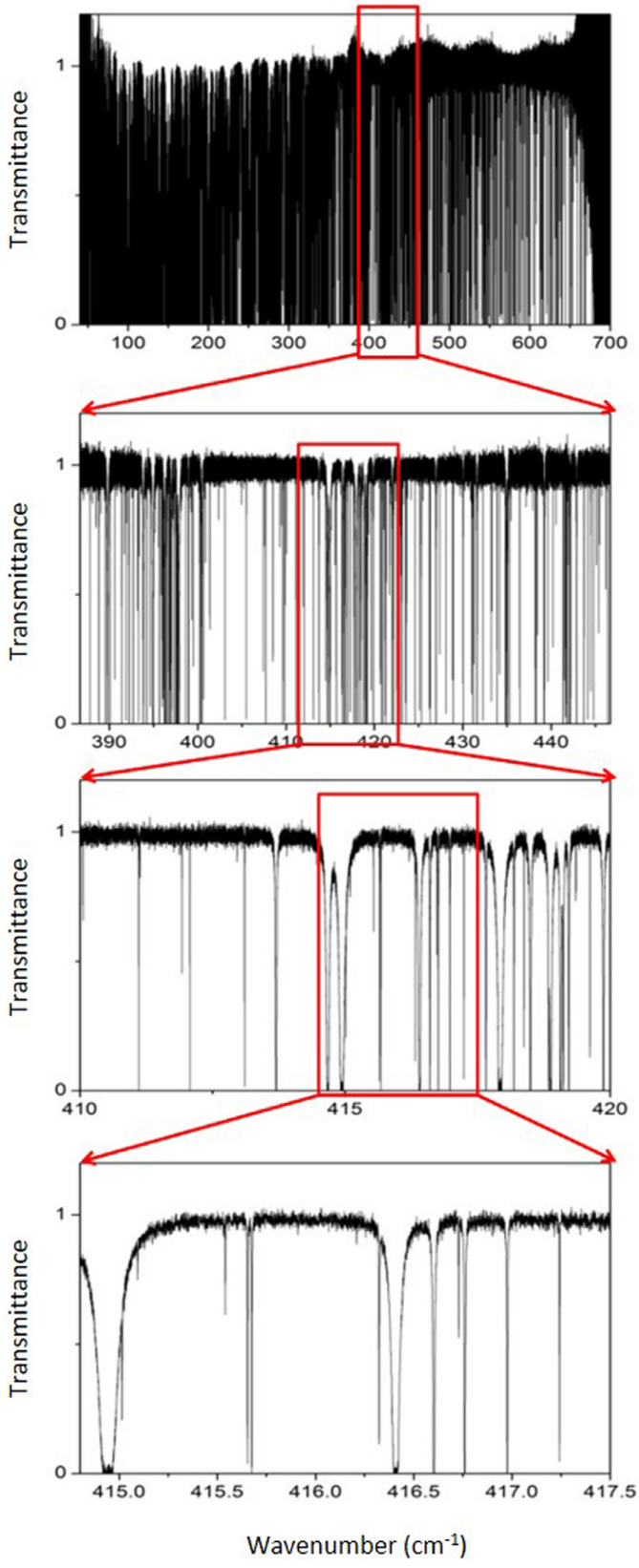


**Fig. 1.** Successive zooms of the room temperature FTS spectrum of water vapour highly enriched in $^{18}O$ recorded at SOLEIL synchrotron ($P = 0.98$ mbar) between 40 and 700 $cm^{-1}$.

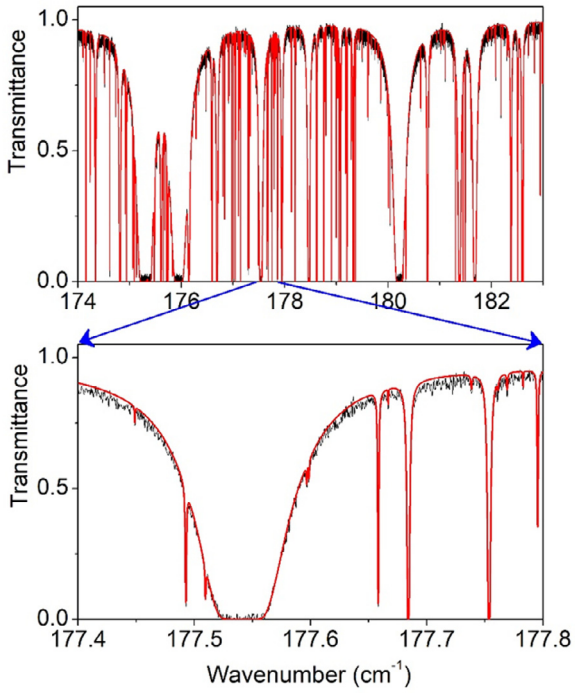


**Fig. 2.** Comparison of the FTS spectrum of water vapour highly enriched in $^{18}O$ near 175 $cm^{-1}$ to a simulation using a Voigt profile as line shape.

**Table 1**
Line-by-line statistics of water transitions assigned between 44 and 678 $cm^{-1}$.

| Molecule | Abundance | NT [a] | $NT_{new}$ [b] | $J_{max}$ $K_{a\ max}$ | Range, $cm^{-1}$ |
|---|---|---|---|---|---|
| $H_2{}^{16}O$ | 0.0523 | 816 | 37 | 19 12 | 44.099 – 673.284 |
| $H_2{}^{18}O$ | 0.9345 | 1206 | 762 | 21 14 | 44.218 – 677.744 |
| $H_2{}^{17}O$ | $9.4 \times 10^{-3}$ | 675 | 318 | 18 12 | 44.218 – 665.558 |
| $HD^{16}O$ | $2.06 \times 10^{-4}$ | 528 | 133 | 18 10 | 46.206 – 558.092 |
| $HD^{18}O$ | $3.51 \times 10^{-3}$ | 1126 | 926 | 21 12 | 44.866 – 645.736 |
| $HD^{17}O$ | $3.72 \times 10^{-5}$ | 363 | 324 | 16 10 | 46.023 – 433.483 |
| $D_2{}^{18}O$ | $3.75 \times 10^{-6}$ | 110 | 38 | 15 10 | 59.554 – 271.653 |
| **Total** | **1.000** | **4824** | **2538** | **21 14** | **44.099 – 677.744** |

Notes.
[a] NT – Number of transitions contributing to the spectrum (including "saturated" lines too strong to be accurately measured).
[b] $NT_{new}$ – Number of transitions which were previously unobserved in absorption or in emission.

dances. The water isotopologue identification included in this preliminary list was used to fix the Doppler broadening according to the mass of the involved isotopologue. We intended to adjust the position, area and Lorentzian width of the different lines but in the case of strongly "saturated" lines, due to the high opacity, the line profile parameters were generally constrained to their default values and only the position and area were fitted. Fig. 2 illustrates the achieved spectrum reproduction. In the case of intermediate intensity lines, (obs. – calc.) residuals corresponding to the noise level (~ 2% of the empty cell transmittance) was generally achieved. This value corresponds to a noise equivalent absorption on the order of $10^{-6}$ $cm^{-1}$ and a detectivity threshold of about $10^{-25}$ cm/molecule for the line intensities.

Overall, line parameters of 5262 absorption features were retrieved. This large dataset includes about 1000 "saturated" water lines too strong to be accurately measured in our experimental conditions. Indeed, the investigated spectral region involves very strong transitions with intensity larger than $10^{-18}$ cm/molecule while the pressure and absorption pathlength conditions of the studied spectrum are suitable for derivation of line intensities in the $5 \times 10^{-25}$ - $8 \times 10^{-23}$ cm/molecule range (see below).

**Table 2**
New energy levels of $H_2{}^{18}O$, $H_2{}^{17}O$, $HD^{18}O$, and $HD^{17}O$ determined from the analysis of the FTS spectrum of water vapour highly enriched in $^{18}O$ between 44 and 678 $cm^{-1}$.

| $J$ | $K_a$ | $K_c$ | Energy[a] | $\delta E$[b] |
|---|---|---|---|---|
| **$HD^{17}O$** | | | | |
| 8 | 7 | 2 | 1286.95798 | 24 |
| 8 | 7 | 1 | 1286.95806 | 25 |
| 9 | 5 | 4 | 1077.48245 | 16 |
| 9 | 6 | 4 | 1237.64510 | 21 |
| 11 | 2 | 9 | 1137.95227 | 23 |
| 11 | 4 | 8 | 1273.25513 | 17 |
| 11 | 4 | 7 | 1282.27792 | 22 |
| 12 | 3 | 9 | 1400.64291 | 32 |
| 12 | 4 | 8 | 1476.06777 | 27 |
| 13 | 4 | 9 | 1687.62496 | 42 |
| 15 | 0 | 15 | 1623.95330 | 60 |
| 15 | 1 | 15 | 1623.95890 | 51 |
| 15 | 1 | 14 | 1807.63052 | 55 |
| 15 | 2 | 14 | 1807.86174 | 57 |
| 16 | 0 | 16 | 1832.90619 | 56 |
| 16 | 1 | 16 | 1832.90869 | 56 |
| **$HD^{18}O$** | | | | |
| 11 | 11 | 1 | 2727.92355 | 17 |
| 11 | 11 | 0 | 2727.92356 | 17 |
| 12 | 10 | 3 | 2625.80073 | 10 |
| 12 | 10 | 2 | 2625.80071 | 11 |
| 12 | 11 | 2 | 2907.45459 | 17 |
| 12 | 11 | 1 | 2907.45459 | 16 |
| 12 | 12 | 1 | 3211.69276 | 20 |
| 12 | 12 | 0 | 3211.69275 | 20 |
| 13 | 10 | 4 | 2821.45430 | 11 |
| 13 | 10 | 3 | 2821.45437 | 11 |
| 13 | 11 | 3 | 3101.84662 | 15 |
| 13 | 11 | 2 | 3101.84664 | 15 |
| 13 | 12 | 2 | 3404.72928 | 20 |
| 13 | 12 | 1 | 3404.72928 | 20 |
| 14 | 9 | 6 | 2776.11040 | 10 |
| 14 | 9 | 5 | 2776.11032 | 11 |
| 14 | 10 | 5 | 3032.03855 | 13 |
| 14 | 10 | 4 | 3032.03955 | 13 |
| 14 | 11 | 4 | 3311.06726 | 15 |
| 14 | 11 | 3 | 3311.06719 | 15 |
| 15 | 6 | 9 | 2390.77152 | 7 |
| 15 | 7 | 8 | 2567.59499 | 8 |
| 15 | 8 | 8 | 2772.56672 | 10 |
| 15 | 8 | 7 | 2772.56729 | 16 |
| 15 | 9 | 7 | 3003.01555 | 13 |
| 15 | 9 | 6 | 3003.01461 | 10 |
| 15 | 10 | 6 | 3257.51792 | 15 |
| 15 | 10 | 5 | 3257.51800 | 14 |
| 16 | 6 | 10 | 2639.47084 | 9 |
| 16 | 7 | 9 | 2813.03401 | 13 |
| 16 | 8 | 9 | 3016.06013 | 12 |
| 16 | 8 | 8 | 3016.07130 | 14 |
| 16 | 9 | 8 | 3244.89230 | 20 |
| 16 | 9 | 7 | 3244.90173 | 15 |
| 17 | 4 | 13 | 2691.62971 | 11 |
| 17 | 5 | 13 | 2746.38188 | 14 |
| 17 | 5 | 12 | 2779.97472 | 13 |
| 17 | 6 | 11 | 2904.61371 | 12 |
| 17 | 7 | 10 | 3073.91144 | 15 |
| 18 | 4 | 15 | 2868.61008 | 14 |
| 19 | 1 | 18 | 2759.48253 | 17 |
| 19 | 2 | 18 | 2759.49883 | 21 |
| 19 | 2 | 17 | 2967.05298 | 17 |
| 19 | 3 | 17 | 2967.43987 | 20 |
| 20 | 0 | 20 | 2782.54227 | 23 |
| 20 | 1 | 20 | 2782.54232 | 23 |
| 20 | 1 | 19 | 3029.29136 | 24 |
| 20 | 2 | 19 | 3029.29996 | 20 |
| 21 | 0 | 21 | 3051.90805 | 26 |
| 21 | 1 | 21 | 3051.90800 | 26 |
| **$H_2{}^{17}O$** | | | | |
| 12 | 11 | 2 | 3493.27691 | 64 |
| 12 | 11 | 1 | 3493.27731 | 66 |
| 12 | 12 | 1 | 3744.31027 | 75 |
| 12 | 12 | 0 | 3744.31067 | 73 |
| 13 | 7 | 7 | 2918.03362 | 46 |
| 13 | 8 | 6 | 3116.43172 | 54 |
| 13 | 9 | 5 | 3333.91518 | 58 |
| 13 | 9 | 4 | 3333.91904 | 44 |
| 13 | 10 | 4 | 3566.86888 | 63 |
| 13 | 10 | 3 | 3566.86799 | 50 |
| 13 | 11 | 3 | 3811.88536 | 71 |
| 13 | 11 | 2 | 3811.88481 | 65 |
| 14 | 4 | 10 | 2876.88740 | 34 |
| 14 | 5 | 10 | 2912.22127 | 44 |
| 14 | 5 | 9 | 2979.51743 | 41 |
| 14 | 6 | 9 | 3077.62393 | 51 |
| 14 | 6 | 8 | 3095.29248 | 40 |
| 14 | 7 | 8 | 3255.17281 | 46 |
| 14 | 7 | 7 | 3257.54686 | 45 |
| 14 | 8 | 7 | 3453.37869 | 51 |
| 14 | 9 | 6 | 3671.37911 | 60 |
| 15 | 1 | 14 | 2625.42191 | 48 |
| 15 | 2 | 14 | 2625.43495 | 51 |
| 15 | 2 | 13 | 2866.13932 | 46 |
| 15 | 3 | 13 | 2866.41578 | 47 |
| 15 | 3 | 12 | 3074.19168 | 49 |
| 15 | 4 | 11 | 3239.69214 | 51 |
| 15 | 6 | 9 | 3467.06349 | 51 |
| 15 | 7 | 8 | 3620.21357 | 64 |
| 16 | 1 | 15 | 2945.81632 | 65 |
| 16 | 2 | 15 | 2945.82275 | 61 |
| 16 | 3 | 14 | 3204.28827 | 61 |
| 16 | 4 | 13 | 3432.23621 | 59 |
| 17 | 0 | 17 | 2974.64780 | 77 |
| 17 | 1 | 17 | 2974.65177 | 89 |
| 17 | 1 | 16 | 3283.81730 | 76 |
| 17 | 2 | 16 | 3283.82057 | 74 |
| 17 | 2 | 15 | 3559.46121 | 71 |
| 18 | 0 | 18 | 3311.98363 | 97 |
| 18 | 1 | 18 | 3311.97966 | 86 |
| 18 | 2 | 17 | 3639.33094 | 84 |
| **$H_2{}^{18}O$** | | | | |
| 15 | 5 | 11 | 3257.12317 | 8 |
| 16 | 1 | 15 | 2939.95141 | 10 |
| 16 | 3 | 13 | 3424.23366 | 11 |
| 16 | 4 | 12 | 3612.34609 | 11 |
| 16 | 5 | 11 | 3749.54756 | 12 |
| 16 | 6 | 10 | 3859.76914 | 10 |
| 16 | 8 | 8 | 4185.60745 | 13 |
| 17 | 2 | 16 | 3277.27565 | 12 |
| 17 | 2 | 15 | 3552.56928 | 9 |
| 17 | 3 | 15 | 3552.63498 | 12 |
| 17 | 3 | 14 | 3796.19838 | 9 |
| 17 | 4 | 14 | 3797.10678 | 14 |
| 17 | 5 | 13 | 4012.43988 | 12 |
| 18 | 0 | 18 | 3305.31389 | 13 |
| 18 | 1 | 18 | 3305.31308 | 11 |
| 18 | 1 | 17 | 3632.07157 | 13 |
| 18 | 2 | 17 | 3632.07254 | 11 |
| 18 | 2 | 16 | 3924.35214 | 13 |
| 18 | 3 | 16 | 3924.38536 | 11 |
| 18 | 3 | 15 | 4184.79228 | 16 |
| 18 | 4 | 15 | 4185.28138 | 11 |
| 18 | 5 | 14 | 4416.22560 | 11 |
| 18 | 15 | 3 | 6806.97939 | 120 |
| 19 | 0 | 19 | 3659.47265 | 13 |
| 19 | 1 | 19 | 3659.47360 | 15 |
| 19 | 1 | 18 | 4004.24664 | 13 |
| 19 | 2 | 18 | 4004.24772 | 15 |
| 19 | 2 | 17 | 4313.21925 | 12 |
| 19 | 3 | 17 | 4313.23774 | 15 |
| 20 | 0 | 20 | 4031.03352 | 17 |
| 20 | 1 | 20 | 4031.03257 | 16 |
| 20 | 1 | 19 | 4393.69352 | 17 |
| 20 | 2 | 19 | 4393.69394 | 14 |
| 21 | 0 | 21 | 4419.88437 | 17 |
| 21 | 1 | 21 | 4419.88532 | 19 |

Notes.
[a] Term energy in $cm^{-1}$.
[b] Statistical uncertainty in $10^{-5}$ $cm^{-1}$.

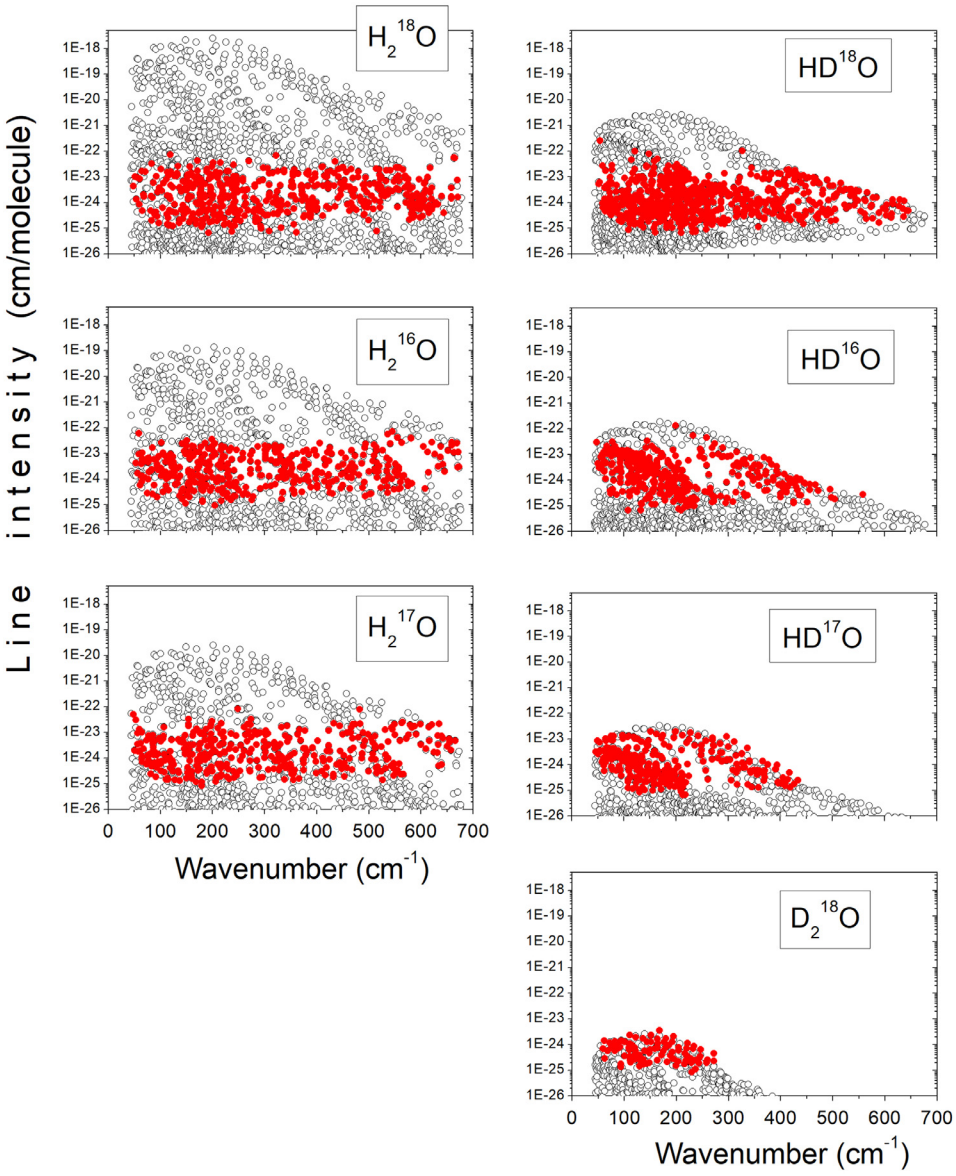


**Fig. 3.** Overview of the presently assigned transitions for the different water isotopologues between 44 and 678 $cm^{-1}$. The plotted observations (red points) are limited to "unsaturated" lines for which line parameters could be reliably determined. Open circles correspond to the HITRAN2016 line list except for $D_2{}^{18}O$, absent in the HITRAN database, for which the predictions based on Schwenke and Partridge calculations [8,9] were used. (For interpretation of the references to colour in this figure legend, the reader is referred to the web version of this article.)

## 3. Rovibrational assignments

The rovibrational assignments were performed using literature results as well as calculated line lists based on the results of Schwenke and Partridge (SP) [8,9]. 4610 lines were assigned to 4824 transitions of seven water isotologues (some absorption features correspond to several transitions-see **Table 1**). In addition, on the basis of the HITRAN2016 database [12], 100 lines were assigned to transitions of HF, $NH_3$, $^{12}C^{16}O_2$, and $^{12}C^{18}O_2$ present as impurities in the sample, with estimated relative concentration of 1, 2, 10 and 7 ppm, respectively (Note the strong $^{18}O$ enrichment of $CO_2$ probably due to oxygen atom exchanges between $^{18}O$ enriched water vapour and natural carbon dioxide). 552 lines with intensity below $8.3 \times 10^{-25}$ cm/molecule remain unassigned. The relative abundances of the different water isotopologues were estimated from the ratio of the measured line intensities to their calculated values [46–51].

**Fig. 3** shows an overview of the "unsaturated" assigned lines for the different isotopologues. The number of assigned transitions, maximum values of rotational numbers and spectral range are given in **Table 1**. The number of newly observed transitions included in the table indicates that new transitions are observed for the seven isotopologues, in particular the main one, $H_2{}^{16}O$, although its relative abundance was limited to about 5% in the used water sample. For the $H_2{}^{18}O$ molecule, the observed lines are rotational transitions within the ground vibrational state or within the (010) and (020) bending states (vibrational states are labelled $(V_1V_2V_3)$ where $V_1$, $V_2$ and $V_3$ are the quantum numbers corresponding to the symmetric stretch, bending and antisymmetric stretch, respectively). For the $H_2{}^{16}O$, $H_2{}^{17}O$, $HD^{16}O$ and $HD^{18}O$ isotopologues, only rotational transitions within the (000) and (010) states are detected while for the least abundant $HD^{17}O$ and $D_2{}^{18}O$ species, only ground state rotational transitions were assigned.

We provide as supplementary material the fitted parameter values of 3625 lines, which were reliably determined, thus excluding

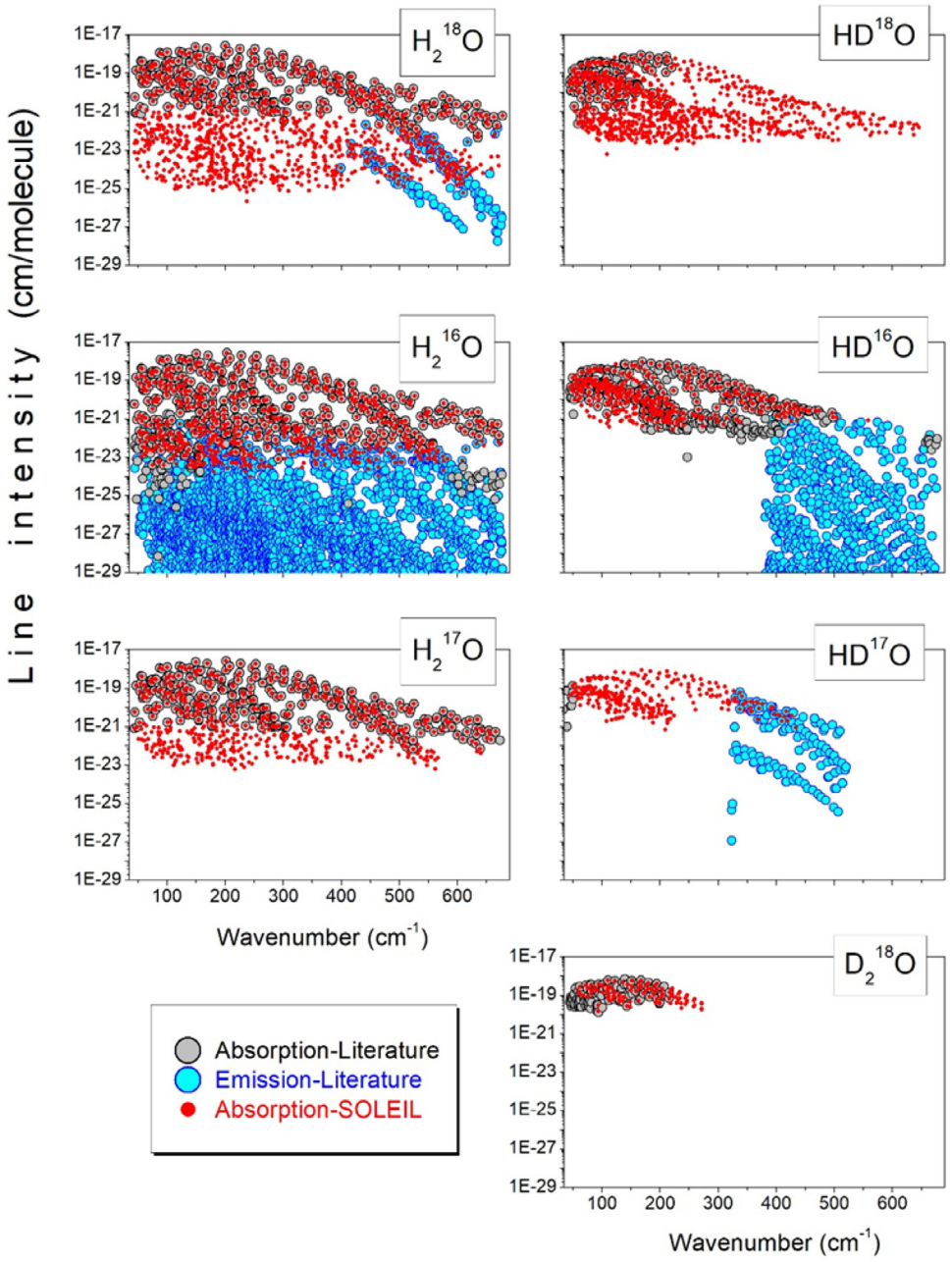


**Fig. 4.** Overview comparison of the present observations (red points) to previous literature data. Transitions from the literature observed by absorption and emission spectroscopy are indicated by grey and blue circles, respectively. For the sake of the comparison, we have associated an absorption line intensity to the emission data. Line intensities correspond to the pure species (100% abundance). (For interpretation of the references to colour in this figure legend, the reader is referred to the web version of this article.)

many "saturated" lines. The position comparison presented below applies to this set of transitions.

Following the exhaustive review of the literature presented in the next paragraph, 35, 41, 50, and 16 new energy levels are determined for $H_2{}^{18}O$, $H_2{}^{17}O$, $HD^{18}O$, and $HD^{17}O$, respectively. They are listed in Table 2.

## 4. Comparison to literature

### 4.1. Previous experimental studies

Some years ago, an IUPAC task group performed an exhaustive review of the experimental investigations of the absorption and emission spectra of the various water isotopologues [52–55]. Each of the IUPAC-TG report includes a table listing the studies available at that time and for each work, the spectral range, the number of reported transitions and the main experimental characteristics. Most of the available experimental data in our region of interest have been obtained by FTS. In particular, several FTS emission spectra provided a considerable amount of observations which should be used with caution because emission line positions are in general less accurate as they suffer from frequent line overlapping and significant Doppler broadening in the case of hot spectra. Overall, most of the previous absorption studies are not recent and limited to less than one hundred lines. This is due to the fact that, all literature works but Ref. [36] used natural water or a

**Table 3**
HITRAN2016 water contents between 44 and 678 $cm^{-1}$.

| Isotopologue | Abundance | Number of transitions | Intensity cut-off (cm/molecule) | References | |
|---|---|---|---|---|---|
| | | | | Position | Intensity |
| $H_2{}^{16}O$ | 0.997317 | 6551 | $1.026 \times 10^{-32}$ | [54,58,59] | [46-49] |
| $H_2{}^{18}O$ | 0.00199983 | 2261 | $1.350 \times 10^{-31}$ | [52,60,61] | [50] |
| $H_2{}^{17}O$ | 0.000371884 | 1832 | $2.020 \times 10^{-31}$ | [50,61] | [50] |
| $HD^{16}O$ | 0.000310693 | 4363 | $1.473 \times 10^{-31}$ | [51] | [51] |
| $HD^{18}O$ | 0.000000623003 | 1824 | $1.500 \times 10^{-31}$ | [51,62] | [51] |
| $HD^{17}O$ | 0.000000115853 | 1403 | $1.576 \times 10^{-31}$ | [51,62] | [51] |
| $D_2{}^{16}O$ | 0.000000024197 | 3534 | $2.301 \times 10^{-34}$ | [51,62] | [51] |
| **Total** | **1.000** | **21,768** | | | |

**Table 4**
Line position comparison with HITRAN2016 [12].

| Molecule | *NT* [a] | $\delta\nu_{max}$ ($10^{-3}$ $cm^{-1}$) | $\delta\nu$ ($10^{-3}$ $cm^{-1}$) [b] | | | |
|---|---|---|---|---|---|---|
| | | | $\delta\nu<0.1$ | $0.1\leq\delta\nu<0.5$ | $0.5\leq\delta\nu<1.0$ | $\delta\nu\geq1.0$ |
| $H_2{}^{16}O$ | 604 | 0.57 | 399 | 201 | 4 | |
| $H_2{}^{18}O$ | 734 | 43.96 | 191 | 295 | 103 | 145 |
| $H_2{}^{17}O$ | 619 | 35.51 | 241 | 202 | 52 | 124 |
| $HD^{16}O$ | 504 | 3.04 | 275 | 211 | 14 | 4 |
| $HD^{18}O$ | 984 | 152.54 | 411 | 369 | 101 | 103 |
| $HD^{17}O$ | 356 | 117.21 | 43 | 180 | 66 | 67 |
| **Total** | **3801** | **152.54** | **1560** | **1458** | **340** | **546** |

Notes.
[a] NT – number of transitions.
[b] Absolute value of the ($\nu_{meas}$.- $\nu_{IUPAC}$) position difference in $10^{-3}$ $cm^{-1}$ unit.

moderated isotopic enrichment in $^{18}O$ while a water vapour highly enriched in $H_2{}^{18}O$ and a long absorption pathlength are presently used. The large amount of newly measured transitions is illustrated in **Fig. 4** where previous observations by absorption and emission spectroscopy are distinguished. In order to give an overview of the available transition wavenumbers, we have associated a line intensity (HITRAN values scaled to 100% abundance for each isotopologue) to all the wavenumbers reported in the literature both in absorption and in emission. Compared to previous absorption studies, a considerable gain is noted for all the isotopologues but $H_2{}^{16}O$ and $HD^{16}O$. In particular, the present measurements lower by four orders of magnitude (from $10^{-21}$ to $10^{-25}$ cm/molecule), the detectivity threshold of $H_2{}^{18}O$ lines and a gain of two orders of magnitude is noted for $H_2{}^{17}O$ and $HD^{18}O$. Previous $HD^{17}O$ measurements were practically absent in this spectral region.

Below, we give a brief updated summary of the present knowledge for the various isotopologues in the region of interest (44–678 $cm^{-1}$).

The most extensive study of $H_2{}^{16}O$ absorption lines in the region was reported by Kauppinen et al. [14] in 1978. 382 pure rotational transitions and 17 rotational transitions of the $\nu_2$-$\nu_2$ band were reported. Later, 233 additional rotational transitions in absorption were reported in Refs. [15–25]. Besides, hot emission spectra provided a high number of rotational and rotation-vibration transitions in the ground and 15 excited vibrational states [26–32]. Overall, 2868 different rotational transitions were reported in Refs. [14–32] within the ground and first excited ($V_2$=1) vibrational states.

#### 4.1.1. $H_2{}^{18}O$ and $H_2{}^{17}O$

The literature data concerning these minor isotopologues is limited. In 1977, Winther measured 121 and 48 pure rotational transitions of $H_2{}^{18}O$ and $H_2{}^{17}O$, respectively, by absorption FTS in natural water vapour below 501 $cm^{-1}$ [33]. Later, 255 absorption transitions were reported for $H_2{}^{18}O$ in Refs. [14,15,17,21,34–36]. Note that only one transition ($3_{2\,2}$ – $3_{1\,3}$ at 73.31376 $cm^{-1}$) was reported by Johns [17] for the first excited state ($V_2$=1). Finally, Mikhailenko et al. [37] assigned 127 $H_2{}^{18}O$ emission lines to 144 transitions in the 399 – 677 $cm^{-1}$ region. 36 of these 144 transitions belong to the $\nu_2$-$\nu_2$ band. Overall, 498 rotational absorption and emission transitions in the (000) and (010) states were reported in Refs. [14,15,17,21,33–37] for $H_2{}^{18}O$. As for $H_2{}^{17}O$, all the 364 transitions known in the far-IR range are pure rotational transitions [14,15,17,21,33–36].

#### 4.1.2. $HD^{16}O$

Only four high resolution studies of $HD^{16}O$ absorption were reported in the studied frequency range. Sixty pure rotational transitions were reported in 1978 by Kauppinen et al. [14] between 152 and 419 $cm^{-1}$. Later, Johns [17], Paso & Horneman [19] and Toth [38] expanded the studied range to 45 – 677 $cm^{-1}$ leading to a total number of 528 transitions. More recently, Janca et al. reported the $HD^{16}O$ emission spectrum above 381 $cm^{-1}$ [39]. Overall, 1168 transitions within the ground and $V_2$=1 vibrational states were reported in our region in Refs. [14,17,19,38,39].

#### 4.1.3. $HD^{18}O$ and $D_2{}^{18}O$

182 and 136 pure rotational transitions between 44 and 220 $cm^{-1}$ were reported by Johns [17] for $HD^{18}O$ and $D_2{}^{18}O$, respectively. More recently, Yu et al. [56] reported accurate measurements of 31 transitions between 50 and 134 $cm^{-1}$ for $HD^{18}O$.

#### 4.1.4. $HD^{17}O$

Up to now, only six transitions of $HD^{17}O$ were measured in absorption [57]. They are located between 46.0 and 50.4 $cm^{-1}$ and show a resolved hyperfine structure due to the nuclear spin of $^{17}O$. In a recent FTS emission study, Mellau et al. [40] assigned 189 transitions to 169 emission lines between 320 and 520 $cm^{-1}$. These measurements provided an extended set of the energy levels of the ground and first excited ($V_2$=1) states up to $J_{max}=17$ and $K_{a\ max}=13$.

**Table 5**
Line position comparison with values calculated using the IUPAC-TG energy levels.

| Molecule | *NT* [a] | *NTO* [b] | $\delta\nu_{max}$ ($10^{-3}$ cm$^{-1}$) | $\delta\nu$ ($10^{-3}$ cm$^{-1}$) [d] $\delta\nu<0.1$ | $0.1\leq\delta\nu<0.5$ | $0.5\leq\delta\nu<1.0$ | $\delta\nu\geq1.0$ |
|---|---|---|---|---|---|---|---|
| $H_2{}^{16}O$ | 604 | 0 | 7.43 | 208 | 286 | 76 | 34 |
| $H_2{}^{18}O$ | 734 | 43 | 39.61 | 189 | 294 | 102 | 106 |
| $H_2{}^{17}O$ | 619 | 49 | 34.98 | 248 | 202 | 49 | 71 |
| $HD^{16}O$ | 504 | 0 | 1.06 | 275 | 212 | 13 | 4 |
| $HD^{18}O$ | 984 | 277 | 29.61 [c] | 105 | 284 | 131 | 187 |
| $HD^{17}O$ | 356 | 174 | 36.24 | 45 | 81 | 30 | 26 |
| $D_2{}^{18}O$ | 110 | 0 | 2.83 | 31 | 63 | 7 | 9 |
| **Total** | **3911** | **543** | **39.61** [c)] | **1101** | **1422** | **408** | **437** |

Notes.
[a] NT – number of transitions.
[b] NTO – number of transitions that could not be calculated for IUPAC energy levels [52,53].
[c] Excluding the 14 $_{3\,11}$ – 13 $_{2\,12}$ rotation transition ($\nu_{OBS}$ = 438.44685 cm$^{-1}$ while $\nu_{IUPAC}$ = 195.91293 cm$^{-1}$ (see Text).
[d] Absolute value of the ($\nu_{OBS}$ - $\nu_{IUPAC}$) position difference in $10^{-3}$ cm$^{-1}$ unit.

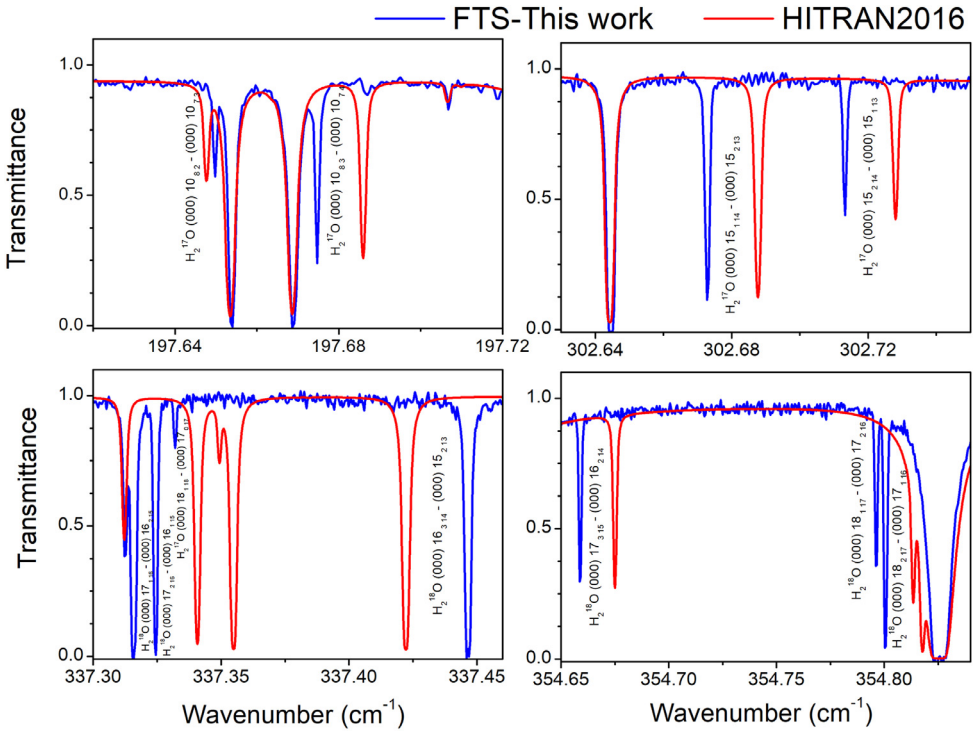


**Fig. 5.** Comparison of the recorded spectrum to a simulation based on the HITRAN2016 database in the same experimental conditions.

### 4.2. HITRAN database

**Table 3** summarizes the contents of the HITRAN2016 water line list [12] in the 44–678 cm$^{-1}$ region. 21,768 transitions of seven isotopologues $H_2{}^{16}O$, $H_2{}^{18}O$, $H_2{}^{17}O$, $HD^{16}O$, $HD^{18}O$, $HD^{17}O$, and $D_2{}^{16}O$ in natural abundance are listed with intensity cut-offs ranging between $2.3\times10^{-34}$ and $2.0\times10^{-31}$cm/molecule depending on the species. The last column of the table gives the source of the HITRAN2016 line positions and line intensities. For all but the main isotopologue, line intensities are *ab initio* values while line positions were calculated from IUPAC-TG energy levels when available or, otherwise, from *ab initio* energy levels. In the case of $H_2{}^{16}O$, 2507 rotation and rotation-vibration transitions in the five lowest vibration states - (000), (010), (020), (100), and (001) - originate from an effective operator approach [46,49,58,59]. For transitions involving other vibrational states, HITRAN line parameters were obtained in the same way as for the minor isotopologues (see Section 2.1 of Ref. [12]).

The systematic comparison of our observations to HITRAN line list revealed that six rotational transitions of $H_2{}^{18}O$ with $J > 17$, observed in our spectrum, are missing in the HITRAN list. Ninety-two rotational transitions of $H_2{}^{18}O$, $H_2{}^{17}O$ and $HD^{18}O$ are provided with incomplete or erroneous assignments. The list of $H_2{}^{18}O$ missing lines and the corrected assignments are provided as Supplementary Material.

**Table 4** summarizes the results of the systematic comparison of our measured line positions to HITRAN values. The comparison applies to lines "unsaturated" in our spectrum (see **Fig. 3**). Due to an extremely small natural relative abundance, $D_2{}^{18}O$ transitions are not included in the HITRAN list. **Table 4** gives the number of transitions corresponding to different ranges of deviations. Overall, a very good agreement is observed for $H_2{}^{16}O$ and to a less extend for $HD^{16}O$. This is not the case for the $H_2{}^{18}O$, $H_2{}^{17}O$, $HD^{18}O$ and $HD^{17}O$ species which show a significant fraction of positions deviating by more than $10^{-3}$ cm$^{-1}$. Maximum deviations correspond to *ab initio* values from Refs. [50,51] and exceed 0.03 cm$^{-1}$ for $H_2{}^{18}O$

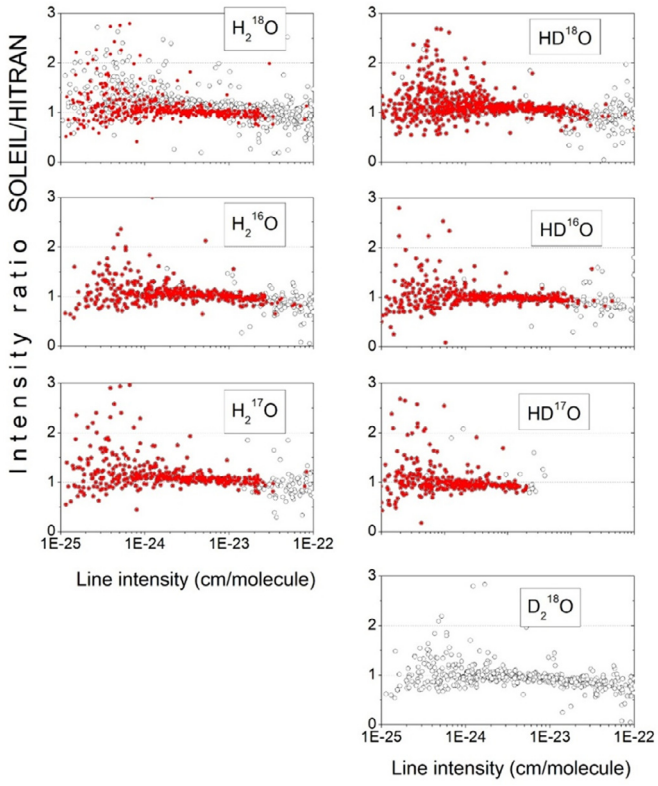


**Fig. 6.** Ratios of measured and HITRAN line intensities *versus* experimental intensity values (for $D_2{}^{18}O$, SP calculated values [8,9] are used instead of HITRAN values [12]). The average intensity ratio was fixed close to unity, by scaling the HITRAN (or SP) intensity values according to the abundance values given in Table 1. The more reliable ratios corresponding to "unsaturated" lines are highlighted (red dots). (For interpretation of the references to colour in this figure legend, the reader is referred to the web version of this article.)

and $H_2{}^{17}O$ and 0.11 $cm^{-1}$ for $HD^{18}O$ and $HD^{17}O$. **Fig. 5** shows a comparison of our FTS spectrum to an HITRAN simulation in the experimental conditions of the recordings for several spectra intervals where HITRAN data deviate importantly from the observations.

The ratios of measured and HITRAN line intensities were used to determine the isotopologue abundance in our sample except for the $D_2{}^{18}O$, absent in the HITRAN list, for which the calculated SP intensities [8,9] were used. The obtained ratios are plotted in **Fig. 6** *versus* the measured line intensities. In order to get an average intensity ratio of unity, the reference intensity values (HITRAN or SP) were scaled according to the abundance values given in **Table 1**. The more reliable sets of ratios corresponding to "unsaturated" lines are highlighted. Overall, the achieved agreement is reasonable. Large errors in the retrieval of the experimental line intensities are believed to be responsible of the observed outliers.

### *4.3. IUPAC task group*

The energy levels recommended by the IUPAC-TG [52–55] have been used to calculate the line centers of our measured transitions. The comparison (**Table 5**) applies to the same set of unsaturated lines as for the HITRAN comparison (**Table 4**). Similarly to the HITRAN comparison, **Table 5** gives the number of transitions corresponding to different ranges of deviations. The considered observed transitions of $H_2{}^{18}O$, $H_2{}^{17}O$, $HD^{18}O$, and $HD^{17}O$ involve 503, 329, 415 and 187 energy levels, respectively. For these four species, the maximum position differences are on the order of 0.03 $cm^{-1}$ and a total of 543 IUPAC positions could not be calculated because they involve levels absent in the IUPAC-TG datasets. More than 10% of the compared line positions deviate by more than $10^{-3}$ $cm^{-1}$ *i.e.* by more than ten times the accuracy of our reported line positions, suggesting that the IUPAC values of the involved energy levels should be significantly corrected. Note that for $HD^{18}O$, we excluded from **Table 5**, the largest position difference corresponding to the $14_{3\,11} - 13_{2\,12}$ transition ($\nu_{OBS} = 438.44685$ $cm^{-1}$ while $\nu_{IUPAC} = 195.91293$ $cm^{-1}$). This error is due to the fact that the upper energy level at 1592.7268 $cm^{-1}$ in the IUPAC energy data set [53] is assigned to the (000) $14_{3\,11}$ level and not to the level (000) $14_{1\,13}$. In fact, this is a result of erroneous assignments of three $\nu_3$ transitions in Ref. [63]. The transitions at 3457.1689, 3482.6769, 3483.1638 $cm^{-1}$ assigned in Ref. [63] as $13_{1\,12} - 14_{1\,13}$, $13_{3\,10} - 14_{3\,11}$ and $13_{2\,12} - 14_{3\,11}$, respectively, should be assigned to $13_{3\,10} - 14_{3\,11}$, $13_{1\,12} - 14_{1\,13}$ and $13_{2\,12} - 14_{1\,13}$, respectively.

## 5. Concluding remarks

The knowledge of the absorption spectrum of water vapour, in particular of the minor isotopologues, has been significantly improved in the range of the rotational band, on the basis of a FTS spectrum highly enriched in $^{18}O$ recorded at the AILES beam line of the SOLEIL synchrotron. The quality of the recorded high resolution spectrum benefitted from the high photon flux and large spectral coverage provided by the synchrotron source. The use of a 151.75 m absorption pathlength allows for the detection of 2538 new transitions of seven water isotopologues ($H_2{}^{18}O$, $H_2{}^{16}O$, $H_2{}^{17}O$, $HD^{18}O$, $HD^{16}O$, $HD^{17}O$, $D_2{}^{18}O$). Overall, one hundred and forty-two energy levels were newly determined for $H_2{}^{18}O$, $H_2{}^{17}O$, $HD^{18}O$, and $HD^{17}O$. In addition, for a large fraction of previously measured transitions (in particular those derived from emission spectra), the line position accuracy (about $10^{-4}$ $cm^{-1}$) is significantly improved. The systematic comparison to the HITRAN2016 database and to the position values derived from the IUPAC-task energy levels reveals a significant number of inaccuracies. Considering that the observed transitions involve the lowest vibrational states of most of the water vapour transitions, the energy levels corrections evidenced in the present study will propagate to a large number of energy values of excited vibrational levels.

*Note added to the proofs*: We have become aware of the (effective Hamiltonian) modelling of the $H_2{}^{18}O$ spectrum up to the first triad and $J$=17 published by Coudert and Chélin [J Mol Spectrosc 2016;326;130–135] thus including our region of interest. The comparison of our experimental positions to those reported in this work has been performed. Overall, positions calculated by Coudert and Chélin show a significantly better agreement to our measurements than those of the HITRAN2016 list. Nevertheless, a number of deviations (up to 0.01 $cm^{-1}$) are noted in particular for the highest J levels of the list of Coudert and Chélin. The comparison will be presented and discussed in details in a future contribution.

## Declaration of Competing Interest

The authors declare that they have no known competing financial interests or personal relationships that could have appeared to influence the work reported in this paper.

## CRediT authorship contribution statement

**S.N. Mikhailenko:** Formal analysis. **S. Béguier:** Formal analysis. **T.A. Odintsova:** Investigation, Writing - review & editing. **M.Yu. Tretyakov:** Investigation, Writing - review & editing. **O. Pirali:** Investigation, Writing - review & editing. **A. Campargue:** Formal analysis, Writing - review & editing.

## Acknowledgements

This work became possible due to the Project No 20180347 supported by SOLEIL Synchrotron Team. TAO and MYT acknowledge the support from the joint RFBR-CNRS project No 18–55–16006. SNM activity was supported by the Ministry of Science and Higher Education of the Russian Federation (Project No. AAAA-A17-117021310147-0). The support of the CNRS (France) in the frame of International Research Project SAMIA is acknowledged.

## Supplementary materials

Supplementary material associated with this article can be found, in the online version, at doi:10.1016/j.jqsrt.2020.107105.

## References

[1] Wayne R.P. Chemistry of atmospheres. New York: Oxford University Press; 3rd edn., 2000.
[2] Schröder M, Lockhoff M, Shi L, August T, Bennartz R, Borbas E, et al.. GEWEX water vapor assessment (G-VAP). WCRP Report 16/2017. Geneva, Switzerland: World Climate Research Programme (WCRP); 2017. p. 216.
[3] Bernath PF. The spectroscopy of water vapour: experiment, theory and applications. Phys Chem Chem Phys 2002;4:1501–9. https://doi.org/10.1039/B200372D.
[4] Kerstel ERTh, Meijer HAJ. Optical isotope ratio measurements in hydrology (Chapter 9), in: isotopes in the water cycle: past, present and future of a developing science. In: Aggarwal PK, Gat J, Froehlich K, editors. IAEA hydrology section. Kluwer; 2005. p. 109–24.
[5] Shine KP, Ptashnik IV, Raedel G. The water vapour continuum: brief history and recent developments. Surv Geophys 2012;33:535–55. https://doi.org/10.1007/s10712-011-9170-y.
[6] Tretyakov MYu, Koshelev MA, Serov EA, Parshin VV, Odintsova TA, Bubnov GM. Water dimer and the atmospheric continuum. Physics – Uspekhi 2014;57:1083–98.
[7] Serov EA, Odintsova TA, Tretyakov MYu, Semenov VE. On the origin of the water vapor continuum absorption within rotational and fundamental vibrational bands. J Quant Spectrosc Radiat Transf 2017;193:1–12.
[8] Partridge H, Schwenke DW. The determination of an accurate isotope dependent potential energy surface for water from extensive *ab initio* calculations and experimental data. J Chem Phys 1997;106:4618–39.
[9] Schwenke DW, Partridge H. Convergence testing of the analytic representation of an *ab initio* dipole moment function for water: improved fitting yields improved intensities. J Chem Phys 2000;113:6592–7.
[10] Polyansky OL, Zobov NF, Mizus II, Lodi L, Yurchenko SN, Tennyson J, et al. Global spectroscopy of the water monomer. Phil Trans R Soc Lond A 2012;370:2728–48.
[11] Polyansky OL, Kyuberis AA, Zobov NF, Tennyson J, Yurchenko SN, Lodi L. ExoMol molecular line lists XXX: a complete high-accuracy line list for water. Mon Not R Astron Soc 2018;480:2597–608.
[12] Gordon IE, Rothman LS, Hill C, Kochanov RV, Tan Y, Bernath PF, et al. The HITRAN2016 molecular spectroscopic database. J Quant Spectrosc Radiat Transf 2017;203:3–69.
[13] Jacquinet-Husson N, Armante R, Crépeau N, Chédin A, Scott NA, Boutammine C, et al. The 2015 edition of the GEISA spectroscopic database. J Mol Spectrosc 2016;327:31–72.
[14] Kauppinen J, Karkkainen T, Kyro E. High-resolution spectrum of water vapor between 30 and 720 $cm^{-1}$. J Mol Spectrosc 1978;71:15–45.
[15] Partridge RH. Far-infrared absorption spectra of $H_2{}^{16}O$, $H_2{}^{17}O$, and $H_2{}^{18}O$. J Mol Spectrosc 1981;87:429–37.
[16] Kauppinen J, Jolma K, Hornaman VM. New wave-number calibration tables for $H_2O$, $CO_2$, and OCS lines between 500 and 900 $cm^{-1}$. Appl Opt 1982;21:3332–6.
[17] Johns JWC. High-resolution far infrared (20-350 $cm^{-1}$) spectra of several species of $H_2O$. J Opt Soc Am B 1985;2:1340–54.
[18] Matsushima F, Odashima H, Iwasaki T, Tsunekawa S, Takagi K. Frequency measurement of pure rotational transition of $H_2O$ from 0.5 to 5 THz. J Mol Struct 1995;352:371–8.
[19] Paso R, Horneman VM. High-resolution rotational absorption spectra of $H_2{}^{16}O$, $HD^{16}O$, and $D_2{}^{16}O$ between 110 and 500 $cm^{-1}$. J Opt Soc Am B 1995;12:1813–37.
[20] De Natale P, Lorini L, Inguscio M, Nolt IG, Park JH, Di Lonardo G, et al. Accurate frequency measurements for $H_2O$ and $^{16}O_3$ in the 119-$cm^{-1}$ OH atmospheric window. Appl Opt 1997;36:8526–32.
[21] Toth RA. Water vapor measurements between 590 and 2582 $cm^{-1}$: line positions and strengths. J Mol Spectrosc 1998;190:379–96.
[22] Chen P, Pearson JC, Pickett HM, Matsuura S, Blake GA. Submillimeter-wave measurements and analysis of the ground and $v_2$=1 states of water. Astrophys J Suppl Series 2000;128:371–85.
[23] Horneman VM, Anttila R, Alanko S, Pietila J. Transferring calibration from $CO_2$ laser lines to far infrared water lines with the aid of the $\nu_2$ band of OCS and the $\nu_2$, $\nu_1$-$\nu_2$, and $\nu_1$+$\nu_2$ bands of $^{13}CS_2$: molecular constants of $^{13}CS_2$. J Mol Spectrosc 2005;234:238–54.
[24] Matsushima F, Tomatsu N, Nagai T, Moriwaki Y, Takagi K. Frequency measurement of pure rotational transitions in the $v_2$=1 state of $H_2O$. J Mol Spectrosc 2006;235:190–5.
[25] Cazzolli G, Puzzarini C, Buffa G, Tarrini O. Pressure-broadening of water lines in the THz frequency region: improvements and confirmations for spectroscopic databases. Part II. J Quant Spectrosc Radiat Transf 2009;110:609–18.
[26] Drouin BJ, Yu SS, Pearson JC, Gupta H. Terahertz spectroscopy for space applications: 2.5 – 2.7 THz spectra of HD, $H_2O$ and $NH_3$. J Mol Structure 2011;1006:2–12.
[27] Polyansky OL, Busler JR, Guo B, Zhang K, Bernath PF. The emission spectrum of hot water in the region between 370 and 930 $cm^{-1}$. J Mol Spectrosc 1996;176:305–15.
[28] Polyansky OL, Tennyson J, Bernath PF. The spectrum of hot water: rotational transitions and difference bands in the (020), (100), and (001) vibrational states. J Mol Spectrosc 1997;186:213–21.
[29] Polyansky OL, Zobov NF, Viti S, Tennyson J, Bernath PF, Wallace L. High-temperature rotational transitions of water in sunspot and laboratory spectra. J Mol Spectrosc 1997;186:422–47.
[30] Coudert LH, Pirali O, Vervloet M, Lanquetin R, Camy-Peyret C. The eight first vibrational states of the water molecule: measurements and analysis. J Mol Spectrosc 2004;228:471–98.
[31] Coheur P-F, Bernath PF, Carleer M, Colin R, Polyansky OL, Zobov NF, et al. A 3000 K laboratory emission spectrum of water. J Chem Phys 2005;122:074307.
[32] Yu SS, Pearson JC, Drouin BJ, Martin-Drumel M-A, Pirali O, Vervloet M, et al. Measurement and analysis of new terahertz and far-infrared spectra of high temperature water. J Mol Spectrosc 2012;279:16–25.
[33] Winther F. The rotational spectrum of water between 650 and 50 $cm^{-1}$ $H_2{}^{18}O$ and $H_2{}^{17}O$ in natural abundance. J Mol Spectrosc 1977;65:405–19.
[34] Kauppinen J, Kyro E. High resolution pure rotational spectrum of water vapor enriched by $H_2{}^{17}O$ and $H_2{}^{18}O$. J Mol Spectrosc 1980;84:405–23.
[35] Guelachvili G, Rao KN. Handbook of infrared standards. Orlando FL: Academic Press; 1986.
[36] Matsushima F, Nagase H, Nakauchi T, Odashima H, Takagi K. Frequency measurement of pure rotational transitions of $H_2{}^{17}O$ and $H_2{}^{18}O$ from 0.5 to 5 THz. J Mol Spectrosc 1999;193:217–23.
[37] Mikhailenko SN, Tyuterev VlG, Mellau G. (000) and (010) states of $H_2{}^{18}O$: analysis of rotational transitions in hot emission spectrum in the 400 – 850 $cm^{-1}$ region. J Mol Spectrosc 2003;217:195–211.
[38] Toth RA. HDO and $D_2O$ low pressure, long path spectra in the 600 – 3100 $cm^{-1}$ region. I. HDO line positions and strengths. J Mol Spectrosc 1999;195:73–97.
[39] Janca A, Tereszchuk K, Bernath PF, Zobov NF, Shirin SV, Polyansky OL, Tennyson J. Emission spectrum of hot HDO below 4000 $cm^{-1}$. J Mol Spectrosc 2003;219:132–5.
[40] Mellau GCh, Mikhailenko SN, Tyuterev VlG. Hot water emission spectra: rotational energy levels of the (000) and (010) states of $HD^{17}O$. J Mol Spectrosc 2015;308-309:6–19.
[41] Evenson KM, Jennings DA, Petersen FR. Tunable far-infrared spectroscopy. Appl Phys Lett 1984;44:576–8.
[42] McKellar ARW. High resolution infrared spectroscopy with synchrotron sources. J Mol Spectrosc 2010;262:1–10.
[43] Odintsova TA, Tretyakov MYu, Zibarova AO, Pirali O, Roy P, Campargue A. Far-infrared self-continuum absorption of $H_2{}^{16}O$ and $H_2{}^{18}O$ (15-500 $cm^{-1}$. J Quant Spectrosc Radiat Transf 2019;227:190–200. https://doi.org/10.1016/j.jqsrt.2019.02.012.
[44] Odintsova TA, MYu Tretyakov, Simonova A, Ptashnik I, Pirali O, Campargue A. Measurement and temperature dependence of the water vapor self-continuum in the 70–700 $cm^{-1}$ range. J Mol Structure 2020;1210:128046. https://doi.org/10.1016/j.molstruc.2020.128046.
[45] Toureille M, Béguier S, Odintsova TA, Tretyakov MYu, Pirali O, Campargue A. The $O_2$ far-infrared absorption spectrum between 50 and 170 $cm^{-1}$. J Quant Spectrosc Radiat Transf 2020;242:106709 doi.org//10.1016/j.jqsrt.2019.106709.
[46] Coudert L.H. Université Paris-Sud, private communication (2004).
[47] Barber RJ, Tennyson J, Harris GJ, Tolchenov RN. A high-accuracy computed water line list. Mon Not R Astron Soc 2006;368:1087–94.
[48] Lodi L, Tennyson J, Polyansky OL. A global, high accuracy ab initio dipole moment surface for the electronic ground state of the water molecule. J Chem Phys 2011;135:034113.
[49] Coudert L, Martin-Drumel M-A, Pirali O. Analysis of the high-resolution water spectrum up to the second triad and J=30. J Mol Spectrosc 2014;303:36–41.
[50] Lodi L, Tennyson J. Line lists for $H_2{}^{18}O$ and $H_2{}^{17}O$ based on empirical line positions and *ab initio* intensities. J Quant Spectrosc Radiat Transf 2012;113:850–8.
[51] Kyuberis AA, Zobov NF, Naumenko OV, Voronin BA, Polyansky OL, Lodi L, et al. Room temperature line lists for deuterated water. J Quant Spectrosc Radiat Transf 2017;203:175–85.
[52] Tennyson J, Bernath PF, Brown LR, Campargue A, Carleer MR, Császár AG, et al. IUPAC critical evaluation of the rotational-vibrational spectra of water vapor. Part I. Energy levels and transition wavenumbers for $H_2{}^{17}O$ and $H_2{}^{18}O$. J Quant Spectrosc Radiat Transf 2009;110:573–96.
[53] Tennyson J, Bernath PF, Brown LR, Campargue A, Császár AG, Daumont L, et al. IUPAC critical evaluation of the rotational-vibrational spectra of water vapor. Part II. Energy levels and transition wavenumbers for $HD^{16}O$, $HD^{17}O$, and $HD^{18}O$. J Quant Spectrosc Radiat Transf 2010;111:2160–84.

[54] Tennyson J, Bernath PF, Brown LR, Campargue A, Császár AG, Daumont L, et al. IUPAC critical evaluation of the rotational-vibrational spectra of water vapor. Part III: energy levels and transition wavenumbers for $H_2{}^{16}O$. J Quant Spectrosc Radiat Transf 2013;117:29–58.
[55] Tennyson J, Bernath PF, Brown LR, Campargue A, Császár AG, Daumont L, et al. IUPAC critical evaluation of the rotational-vibrational spectra of water vapor. Part IV: energy levels and transition wavenumbers for $D_2{}^{16}O$, $D_2{}^{17}O$, and $D_2{}^{18}O$. J Quant Spectrosc Radiat Transf 2014;142:93–108.
[56] Yu SS, Pearson JC, Drouin BJ, Miller CE, Kobayashi K, Matsushima F. Terahertz spectroscopy of ground state $HD^{18}O$. J Mol Spectrosc 2016;328:27–31.
[57] Puzzarini C, Cazzoli G, Gauss J. The rotational spectra of $HD^{17}O$ and $D_2{}^{17}O$: experiment and quantum-chemical calculations. J Chem Phys 2012;137:154311.
[58] Lanquetin R, Coudert LH, Camy-Peyret C. High-lying rotational levels of water: an analysis of the energy levels of the five first vibrational states. J Mol Spectrosc 2001;206:83–103.
[59] Flaud J-M, Piccolo C, Carli B, Perrin A, Coudert LH, Teffo J-L, Brown LR. Molecular line parameters for the MIPAS (Michelson Interferometer for Passive Atmospheric Sounding) experiment. Atmos Ocean Opt 2003;16:172–82.
[60] Bubukina II, Zobov NF, Polyansky OL, Shirin SV, Yurchenko SN. Optimized semiempirical potential energy surface for $H_2{}^{16}O$ up to 26000 $cm^{-1}$. Opt Spectrosc 2011;110:160–6.
[61] Kyuberis AA Institute of Applied Physics RAS. Private communication (2016). Based on the updated database of energy levels from Ref. [52].
[62] *Ab initio* values from Ref. [50]
[63] Liu A-W, Du J-H, Song K-F, Wang L, Wan L, Hu S-M. High-resolution Fourier–transform spectroscopy of $^{18}O$ enriched water molecule in the 1080 – 7800 $cm^{-1}$ region. J Mol Spectrosc 2006;237:149–62.